Cell Reports

Supplemental Information

Report

Axon Dynamics during Neocortical Laminar Innervation

Randal A. Hand, Syed Khalid, Edric Tam, and Alex L. Kolodkin

Figure S1

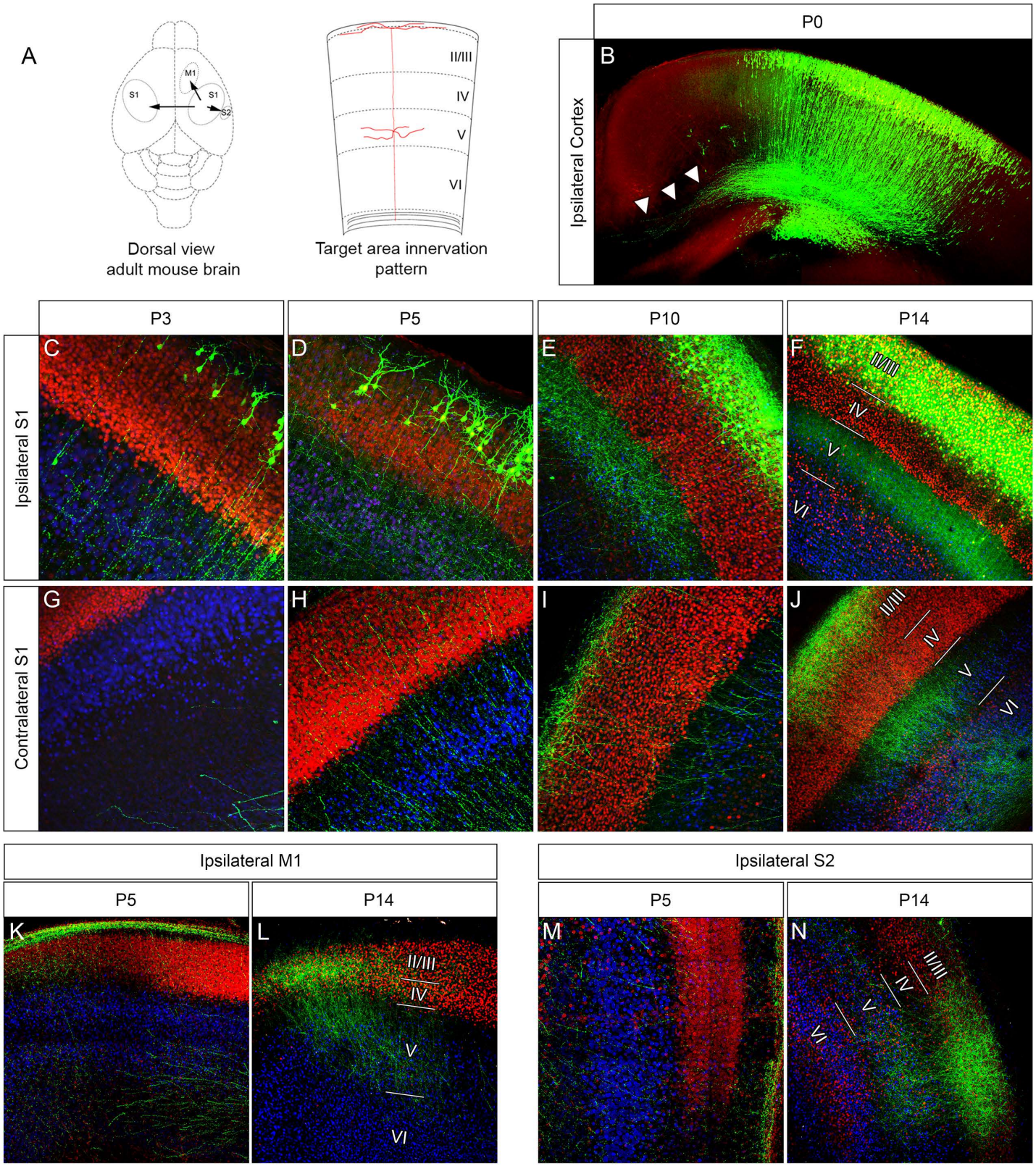
A
M1
S1
S1
S2
Dorsal view
adult mouse brain
II/III
IV
V
VI
Target area innervation
pattern
P0
B
Ipsilateral Cortex
P3
P5
P10
P14
C
D
E
F
II/III
IV
V
VI
Ipsilateral S1
G
H
I
J
Contralateral S1
Ipsilateral M1
Ipsilateral S2
P5
P14
P5
P14
K
L
M
N

Figure S1. Developmental timing of innervation in the cerebral cortex by layer II/III pyramidal neurons from S1, related to Figure 1.

A schematic diagram illustrating the innervation pattern of layer II/III pyramidal neurons in S1 (A). Confocal images of layer II/III pyramidal neurons in S1 labeled by targeted IUE at E15.5 with plasmids encoding eGFP (B–N). Images were taken at time points ranging from P0 to P14 in the areas innervated by S1 layer II/III pyramidal neurons. Brain sections were counter stained with either with DAPI (red, B), or Cux1 (red) and CTIP2 (blue) to demarcate cortical layers II-IV and V, respectively (C–N). At P0 layer II/III pyramidal neurons are completing migration as their axons project towards the corpus callosum (composite panoramic image B, white arrows). In the ipsilateral S1 cortex (C–F), collateral axons begin to form at P3 (C) and a clear axonal plexus may be observed in layer V at P10 (E). The primary axon may be observed entering the contralateral S1 cortex at P3 (G). By P5, axons reach the most superficial layers of the cerebral cortex (H). Terminal arbors of the primary axon are present at P10 (I), and the laminar specific innervation of layers II/III and layer V in the contralateral S1 cortex may be observed by P14 (J). In the ipsilateral M1 cortex, axons from layer II/III S1 pyramidal neurons are present by P5 (K) and laminar specific innervation is observed at P14 (L). Similarly, axons from layer II/III S1 pyramidal neurons we observed in the ipsilateral S2 cortex at P5 (M) and laminar specific innervation is present at P14 (N).

Figure S2

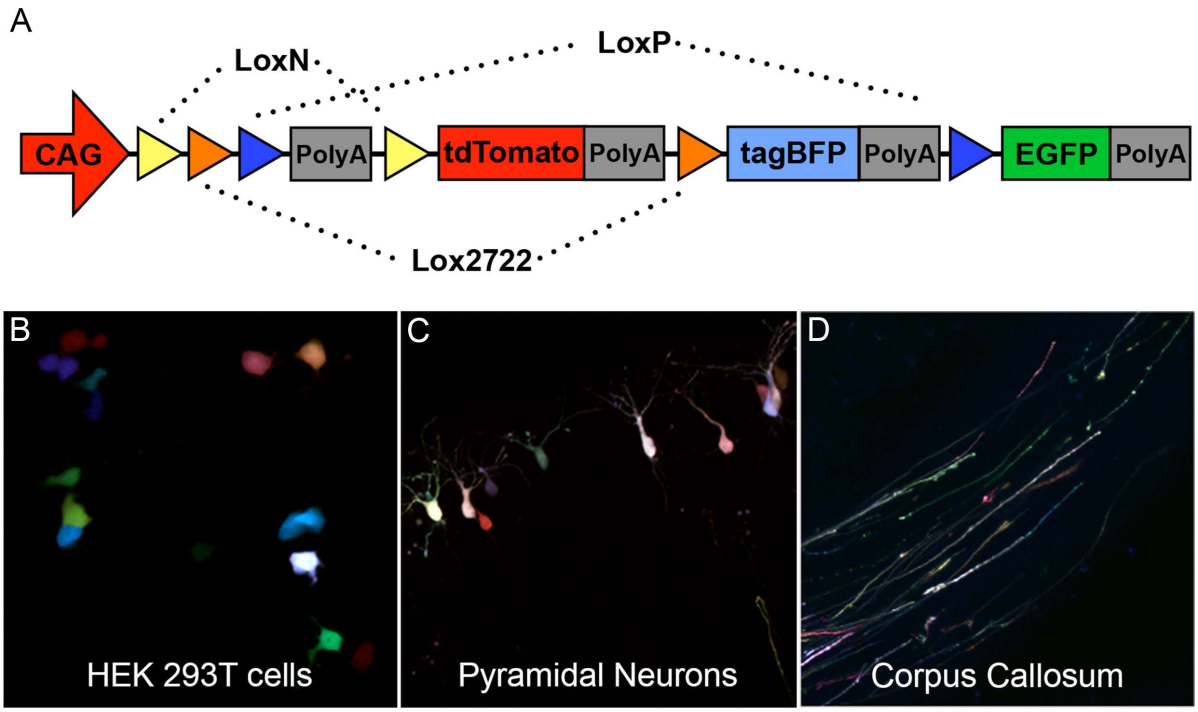

Figure S2. The MAGIC marker plasmid Randbow allows for simultaneous observation of multiple cells, related to Figure 2 and Movie S3.

A schematic diagram of the pCAG-Randbow construct (A). Examples, left to right, of live images from HEK 293T cells transfected with Randbow and Cre plasmids, P4 S1 layer II/III pyramidal neurons labeled by IUE, and axons from S1 layer II/III pyramidal neurons within the corpus callosum (see also Movie S3).

Figure S3

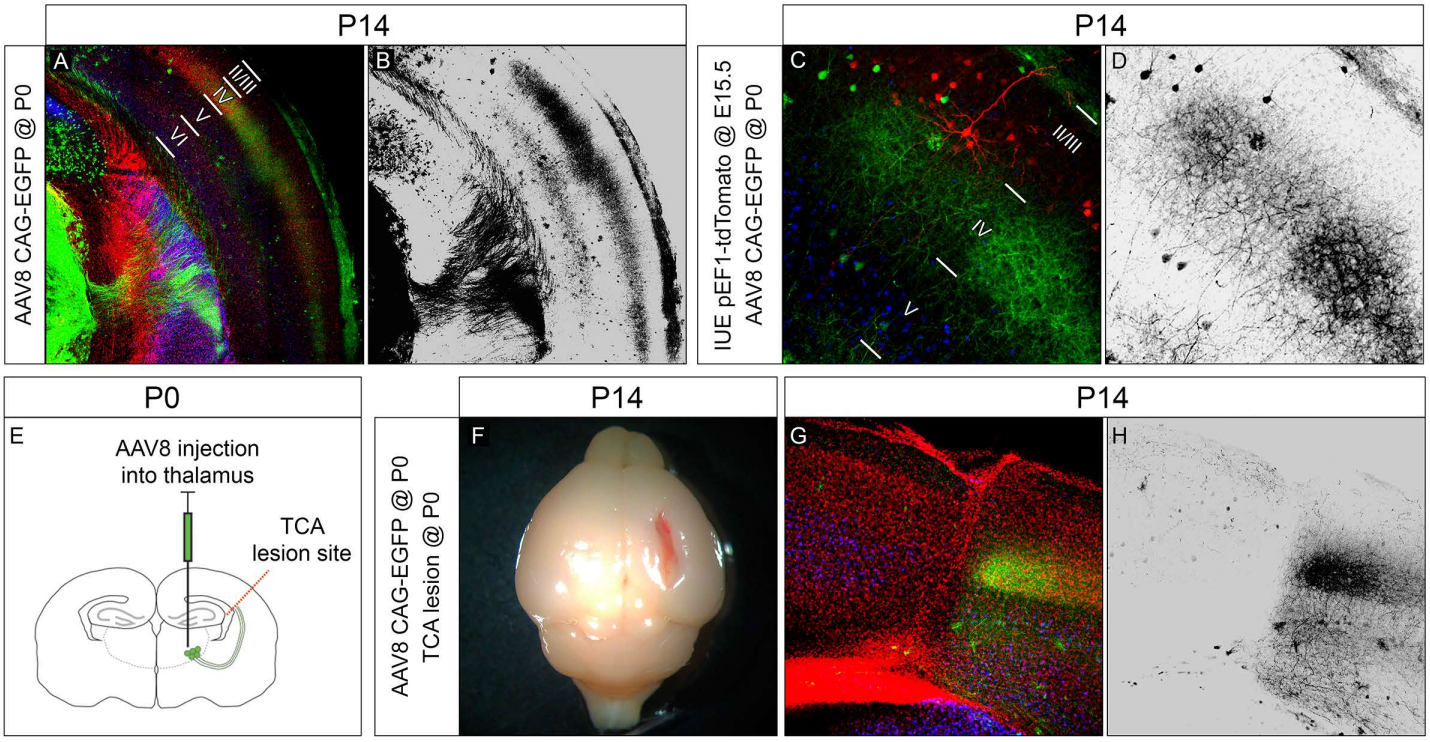

Figure S3. Lesions prevent innervation of S1 by thalamocortical axons, related to Figure 5.

Thalamocortical axons (TCAs) were labeled by injections of high titer AAV8 viruses encoding eGFP into the developing fields of the thalamus at P0 (green: A,C,G; black: B,D,H). The innervation of layer IV and VI by TCAs is visualized in brain sections at P14 (A,B). Brain sections were counter stained with DAPI (red: A,G) and CTIP2 (blue: A,C,G) to identify cortical layers. The juxtaposition of layer II/III pyramidal neurons and TCAs can be observed by introducing plasmids encoding tdTomato into layer II/III pyramidal neurons by IUE (red: C). A schematic illustration of AAV8 injections to label TCAs and of the TCA lesion site (E). Whole mount bright field image of a P14 mouse brain that underwent a TCA lesion at P0 (F). eGFP-labeled TCAs fail to cross lesion sites (G,H).

Figure S4

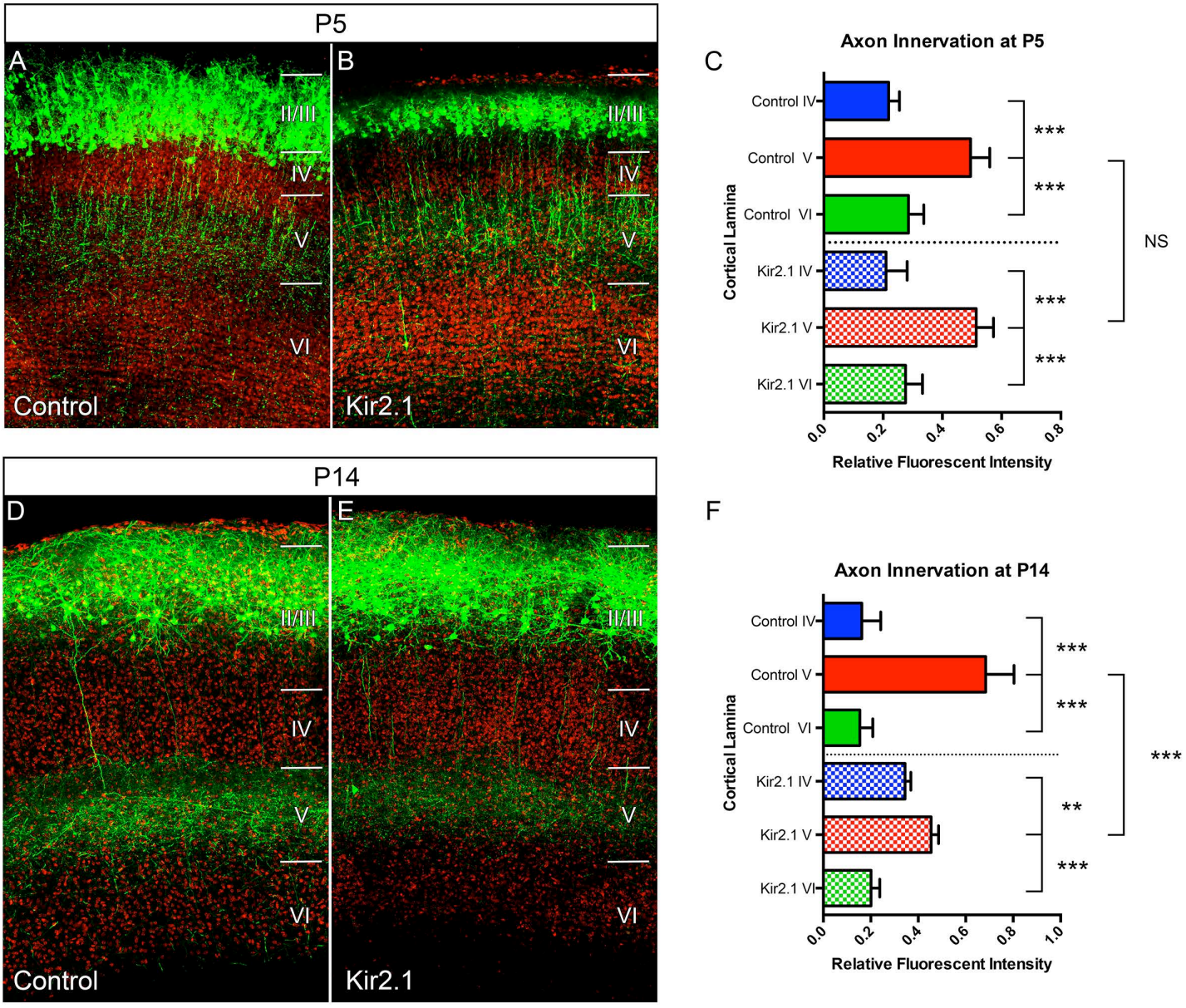

Figure S4. Hyper-polarizing S1 layer II/III pyramidal neurons does not abolish lamina-specific innervation, related to Figure 2.

Plasmids encoding tdTomato and plasmids encoding either IRES-eGFP (control) or Kir2.1-IRES-eGFP were introduced into layer II/III pyramidal neurons by IUE at E15.5. Confocal images of 250μm fixed coronal sections were used to assess laminar-specific

innervation of layer II/III pyramidal neurons at P5 (A,B) and P14 (D,E) by tdTomato fluorescence (green). Brain sections were counterstained with DAPI (red) to determine cortical laminae locations (A,B,D,E). At P5 (C) and at P14 (F) a significant increase in the innervation of layer V, as compared to layers IV and VI, was found within both control and Kir2.1-expressing animals. By two-way ANOVA no significant difference was found between of control and Kir2.1-expressing animals at P5, however a significant difference was found in the ratios of innervation between control and Kir2.1-expressing animals at P14. * Indicates a P value < 0.05. ** indicates a P value < 0.01. *** indicates a P value < 0.001. NS indicates no significance. Error bars denote standard deviation.

Table S1

Cortical Area	Axons arrive	Axon branching is observed	Laminar specific axon plexus
Ipsilateral S1	P0	P3	P10
Contralateral S1	P5	P10	P14
Ipsilateral M1	P5	P10	P14
Ipsilateral S2	P5	P10	P14

Table S1. Summary of innervation by S1 layer II/III pyramidal neurons, related to Figure 1.

Movie S1. Tile scan time-lapse images allow for the visualization of layer II/III pyramidal neurons during initial neural circuit formation, related to Figure 2.
Layer II/III pyramidal neurons from S1 were labeled by IUE of plasmids encoding eGFP (black) at E15.5. A tile scan image consisting of 11 x 8 fields with a 10x objective was taken of a P4 400μm organotypic brain section every hour for 24 hours. Axons from S1 layer II/III pyramidal neurons can be observed navigating to their appropriate targets in the contralateral S1, ipsilateral M1, and ipsilateral S2.

Movie S2. Tile scan time-lapse images beginning at P2.5 reveal initial collateral axon branch dynamics in the ipsilateral S1, related to Figure 2.
Layer II/III pyramidal neurons from S1 were sparsely labeled by IUE of plasmids encoding eGFP (black) at E15.5. A tile scan image was obtained with a 20x objective every hour for 16hrs from a P2.5 400μm organotypic brain section. Short collateral axon branches can be observed emerging and retracting all along the primary axon.

Longer more persistent axon collateral branches can be observed forming within layer V. Red lines depict the average depth of each cortical layer. Cortical layers are denoted by red text.

Movie S3. Multicolor labeling allows collateral axon branches from multiple layer II/III pyramidal neurons to be visualized simultaneously, related to Figure 2.

In order to visualize multiple neurons simultaneously, layer II/III pyramidal neurons were labeled by electroporation of plasmids encoding Cre and plasmids in which Cre recombination results in the expression of either tagBFP, eGFP or tdTomato. Longer, more persistent, collateral axons are formed within layer V. A tile scan image was obtained with a 20x objective every hour for 16hrs from a P2.5 400μm organotypic brain section. White lines depict the average depth of each cortical layer. Cortical layers are denoted by white text.

Movie S4. Time lapse images of filopodia dynamics of primary axons from layer II/III pyramidal neurons in the ipsilateral S1, related to Figure 3.

Layer II/III pyramidal neurons from S1 were sparsely labeled by IUE of plasmids encoding eGFP at E15.5. Filopodia formation and retraction is observed along the entire axon. Images were obtained with a 20x objective every 10 minutes from a P4.5 400μm organotypic brain section.

Movie S5. F-actin dynamics during collateral axon branch formation, related to Figure 4.

Time lapse images of an axon from a layer II/III pyramidal neuron co-labeled with eGFP (green) and the calponin homology domain of utrophin fused to mRFP (magenta), a f-actin biosensor. F-actin dynamics may be observed along the axon shaft and in axon growth cones. Cortical layers are depicted in white. Images were obtained with a 40x NA1.3 oil emersion objective every 2.5 minutes for 8hrs from a P4.5 400μm organotypic brain section.

Supplemental Experimental Procedures

Plasmids. For general labeling of neurons with eGFP (Figures 1 and S1) or tdTomato (Figures 5 and S4), a pCAG-eGFP plasmid at a concentration of 2μg/μl or a pEF1-tdTomato plasmid at a concentration of 1μg/μl were used. The tdTomato plasmid was used at lower concentrations since tdTomato is inherently brighter than eGFP. For sparse labeling with eGFP (Figures 1, 2, 3, and 4; Movies S1 and S3), plasmids encoding Cre-dependent eGFP (pCAG-LSL-eGFP at a concentration of 2μg/μl) and Cre (pCAG-Cre at concentrations ranging between 1-10ng/ul) were co-electroporated (the lower the concentration of the Cre plasmid, the more sparse the labeling with eGFP becomes). To visualize multiple cells simultaneously (Figure S2 and Movie S2), we generated and electroporated a recombination-assisted neural delineation plasmid, pCAG-Randbow, along with the pCAG-Cre plasmid at concentrations of 2μg/μl and 10ng/μl, respectively. pCAG-Randbow was created by optimizing the pCx-Cytobow (a kind gift from Alain Chédotal). This optimization involved inserting a polyA sequence upstream of tdTomato and a loxN sequence downstream of tdTomato to make the expression of tdTomato conditional upon Cre-mediated recombination. We also replaced the Cerulean and Venus fluorophores from pCx-Cytobow with tagBFP and

eGFP fluorophores, whose excitation and emission spectra align better with our imaging system. To label the f-actin cytoskeleton (Figure 6), we electroporated embryos with the pCAG-UtrCh-mRFP plasmid at a concentration of 250ng/µl. In experiments involving the manipulation of intrinsic neural activity, we introduced either a pCAG-IRES-eGFP plasmid as a control or a pCAG-Kir2.1-IRES-eGFP at concentrations of 1µg/µl.

Antibodies. Primary antibodies were diluted in permeabilization buffer as follows: chicken anti-eGFP (Aves, Cat# GFP-1010, RRID: AB_2307313) 1:1000, rabbit anti-Cux1 (SantaCruz Biotechnology, Cat# sc-13024, RRID: AB_2261231) 1:500, rat anti-CTIP2 (AbCam, Cat# ab18465, RRID: AB_2064130) 1:2000, and rabbit anti-mRFP (Clontech, Cat# 632496, RRID: AB_10015246) 1:1000. All Alexa Fluor-conjugated secondary antibodies were used at 1:1000.

Live and fixed imaging. For the low magnification time-lapse images (Figures 2A and 2B; and Movies S1-3), tile scan images were acquired every hour for 16hrs. Figure 2A and Movie S1 were acquired using a 10X EC Plan Neofluar objective NA0.3 (Zeiss). Figures 2B, Movies S2 and S3 were acquired using a 20X Apochromat NA0.8 objective (Zeiss). Higher magnification time-lapse images were acquired using a 20X Apochromat NA0.8 objective (Zeiss) with images were acquired every 10 minutes (Figures 3A; Movie S4) or using a 40X EC Plan Apochromat NA1.3 oil immersion objective (Zeiss) every 2.5 minutes (Figure 4A and Movie S5) for times ranging from 8 to 12 hours. Fixed images were acquired on either a Zeiss LSM510 (MPI Core, JHMI) or a Zeiss LSM700. All live imaging was performed on a Zeiss inverted LSM700 with a Pecon incubation system.

*Image processing and data analysis***.** All images were processed, and time-lapse images compiled, using ImageJ. Student's t-test and ANOVA followed by a Tukey's test were used to compare means across experimental groups as appropriate. Chi squared test and Cochran's Q-test were performed to compare categorical data where appropriate. For descriptive images (Figure 1 and Figure S1) all observations were made from a minimum of 5 animals at all time points. For collateral axon branch analysis (Figures 2), only neurons with axons that could be visualized across the entire cortical wall, and whose axons persisted for a minimum of 8hrs, were analyzed. Data meeting our criteria for analysis in control groups (eGFP expressing neurons; Figure 2) came from 4 independent litters, 5 different brain sections, and a total of 15 different neurons. In the collateral axon branch analysis of Kir2.1-expressing neurons (Figure 2), data from 3 independent litters, 5 different slices, and a total of 15 different neurons were quantified. For filopodia analysis (Figure 3), only neurons whose axons spanned the entire cortical wall and that persisted for at least 4hrs were quantified. The filopodia data were generated from the analysis of 3 independent litters, 14 independent images, 26 axons, and 566 filopodia. Data acquired for the f-actin analysis (Figure 4) were obtained from 4 litters, 5 animals, 6 axons, and 647 pools of f-actin. For the Kir2.1 innervation experiments, areas of equal size were used to measure the fluorescent intensity within each layer (Figure S4). In the Kir2.1 experiments innervation experiments 12 control animals and 12 Kir2.1 expressing animals were quantified (7 animals for each group at P5 and 5 animals for each group at P14). For the corpus callosum lesion and thalamocortical axon lesion experiments, areas of equal size were used to measure the fluorescent intensity within each layer (Figure 5). For the corpus

callosum lesion experiments, 3 control (non-lesioned) animals and 4 lesioned animals were quantified; for the thalamocortical axon lesion experiments 4 control and 4 lesioned animals were quantified.